Chemical effects on the optical band-gap of heavily doped ZnO:M_{III} (M=Al,Ga,In): An investigation by means of photoelectron spectroscopy, optical measurements under pressure, and band structure calculations

J. A. Sans,[1] J. F. Sánchez-Royo,[1,*] A. Segura,[1] G. Tobias,[2] and E. Canadell[3]

[1]*Departamento de Física Aplicada-ICMUV, MALTA Consolider Team, Universidad de Valencia, Edificio de Investigación, c/Dr. Moliner 50, 46100 Burjassot, Valencia, Spain*

[2]*Inorganic Chemistry Laboratory, University of Oxford, South Parks Road, OX1 3QR Oxford, United Kingdom*

[3]*ICMAB, CSIC, Campus de la Universidad Autónoma de Barcelona, 08193 Bellaterra, Barcelona, Spain*

Chemical effects on the conduction-band filling and band-gap renormalization in ZnO thin films doped with group-III elements (Al, Ga, and In) are investigated by means of optical and photoemission experiments and first-principles density-functional calculations. The Fermi-level position, as obtained from ultraviolet photoemission measurements, exhibits a relatively small and positive shift (about 0.4 eV) with respect to the valence band for increasing electron concentrations up to 10^{21} cm^{-3}. The optical gap exhibits a much larger increase for the same concentration range and the total shift appears to be smaller for In-doped ZnO. Absorption measurements under pressure show that the pressure coefficient of the optical gap is correlated with the electron concentration in films, decreasing with increasing electron concentration. As a consequence, the contributions of band filling and band-gap renormalization to the optical-gap shift can be separated on the basis of the different pressure behavior of the physical parameters involved in each effect. Standard models on band-gap narrowing fail to give account of these results. Supercell density-functional calculations show that the conduction band of heavily doped ZnO is modified by the presence of group-III doping elements, which give rise to small gaps in specific points of the Brillouin zone, modifying the conduction band dispersion in the way predicted, in a much simpler approach, by the band-anticrossing model.

PACS number(s): 78.66.Hf, 71.20.Nr, 71.70.−d

I. INTRODUCTION

Zinc oxide (ZnO) is the object of an increasing interest in the last few years owing to its potential applications in ultraviolet (UV) optoelectronic devices,[1,2] transparent conducting oxide (TCO) thin films,[3,4] and spintronics.[5] For the design and realization of ZnO-based devices, one of the most relevant issues is doping. This issue is especially important for the applications of ZnO as TCO, which necessarily involves the heavy doping with trivalent elements from the group III. By means of doping, large conductivities combined with large ranges of transparency in the visible (VIS) and near UV range are so obtained.[6,7] In spite of the quick progress in the quality of epitaxially grown ZnO thin films, there are relatively few papers on some properties or effects, such as band-gap renormalization, that are crucial to understand the behavior of the optical gap (E_g^{op}) of ZnO-based TCO films. The band-gap renormalization in heavily doped ZnO has been the object of some early papers[6,8] and some more recent ones.[9–12] Band-gap renormalization results in a gap narrowing due to exchange interactions in the free-electron gas and electrostatic interactions between free electrons and ionized impurities.[6,13] This band-gap narrowing is not actually observed in the E_g^{op} behavior with doping as it is largely compensated by band filling effects (Burstein-Moss effect)[14,15] which results in the well-known E_g^{op} blueshift in heavily doped semiconductors.[6–8] In all standard models proposed to explain the optical properties of heavily doped ZnO, donor atoms are considered as merely inert agents that control the free carrier population, neglecting the existence of any effect dependent on the chemical nature of the cation.

The present work is devoted to analyze chemical effects on the different mechanisms determining the E_g^{op} shift in ZnO:M heavily doped with elements from the group III (M=Al, Ga, or In). With this purpose, photoemission and optical measurements of the absorption edge have been performed in ZnO thin films doped with Ga and In. The absorption edge of free-standing ZnO:M films has been also measured as a function of pressure. The effects of heavy doping on the electronic structure have been analyzed by means of band structure calculations. The experimental setup is described in Sec. II. Section III is devoted to describe the technical aspects of the band structure calculations. In Sec. IV, the results obtained are presented and discussed. Finally, in Sec. V we present the main conclusions of this work.

II. EXPERIMENT

Targets for pulsed laser deposition (PLD) were prepared from high purity (99.999%) ZnO and Ga$_2$O$_3$ (In$_2$O$_3$) powders with Ga (In) atomic proportion (with respect to the total cation content) from 0.05% to 5%.[16] ZnO:M thin films here studied were prepared by PLD on double-side polished c-oriented sapphire and mica monocrystalline substrates. The PLD system and conditions have been described in Ref. 17.

Ultraviolet photoemission measurements (UPS) were carried out in an ultra-high-vacuum ESCALAB 210 multianalysis system (base pressure 1.0×10^{-10} mbar) from Thermo VG Scientific. Photoelectrons were excited by means of a helium lamp by using both the He I (21.2 eV) and He II (40.8 eV) excitation lines. All spectra obtained have been

referred to the Fermi level (E_F). Previously to these measurements, samples were introduced in the analysis chamber and sputtered by using an Ar$^+$ gun for 15 min, in order to clean the surface. Then, x-ray photoemission measurements were performed to check that the presence of adventitious C on the surface sample was under the detection limit of the experimental setup.

Samples for optical measurements in the diamond-anvil cell were free-standing films that can be easily separated from the mica substrates. For optical absorption measurements in the UV/VIS/near-infrared range under pressure, a sample was placed together with a ruby chip into a 200 μm diameter hole drilled on a 50 μm thick Inconel gasket and inserted between the diamonds of a membrane-type diamond-anvil cell.[18] Methanol-ethanol-water (16:3:1) was used as pressure transmitting medium and pressure was determined through the ruby luminescence linear scale.[19] The optical setup was similar to the one described in Ref. 18. It consists of a deuterium lamp, fused silica lenses, reflecting optics objectives, and an UV-VIS spectrometer, which allows for transmission measurements up to the absorption edge of IIA diamonds (about 5.5 eV).

III. COMPUTATIONAL DETAILS

Band structure calculations were carried out using a numerical atomic orbitals density-functional theory (DFT) approach,[20] which has been developed and designed for efficient calculations in large systems and implemented in the SIESTA code.[21–23] We have used the generalized gradient approximation to DFT and, in particular, the functional of Perdew, Burke, and Ernzerhof.[24] Only valence electrons are considered in the calculation, with the core being replaced by norm-conserving scalar relativistic pseudopotentials[25] factorized in the Kleinman-Bylander form.[26] Nonlinear partial core corrections to describe the exchange and correlations in the core region were used for Zn, Al, Ga, and In.[27] We have used a split-valence double-ζ basis set including polarization orbitals for all atoms, as obtained with an energy shift of 250 meV.[28] The $3d$ electrons of Zn and Ga as well as the $4d$ electrons of In were treated as valence electrons. For Zn we have used a pseudopotential generated using a Zn^{2+} reference configuration[29] and an optimized basis set.[30] We have checked that the crystallographic parameters for ZnO obtained in such way ($a=3.300$ Å, $c=5.297$ Å, and $u=0.381$) are in good agreement with the more accurate plane-wave-type DFT calculations presently available[31] ($a=3.282$ Å, $c=5.291$ Å, and $u=0.379$) and the experimental structure[32] ($a=3.250$ Å, $c=5.200$ Å, and $u=0.382$). For Al, Ga, and In the pseudopotential was generated using a M^{3+} reference configuration. We checked that the structure of the corresponding M$_2$O$_3$ oxides is in good agreement with experimental values. All calculations were carried out using a $3\times3\times2$ supercell in which one of the Zn atoms is substituted by a group-III cation, which would correspond to a doping degree close to the 3%. The energy cutoff of the real space integration mesh was 1600 Ry. The Brillouin zone was sampled using a grid of $(2\times2\times2)$ k points.[33] The structures were fully optimized. We checked that the results were well
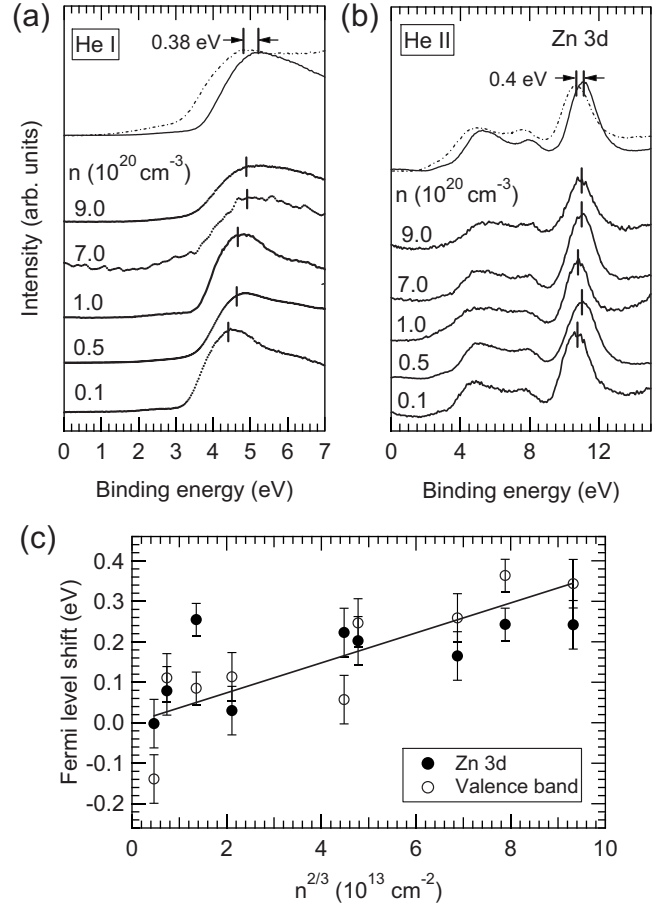
FIG. 1. (a) He I and (b) He II valence-band spectra measured by UPS in ZnO:Ga films prepared with different Ga content. The electron density of each film is indicated on its spectrum. The position of the main features identified has been indicated by solid bars. Top curves in these plots correspond to the spectra measured in a ZnO:Ga 5% film (solid curves) with a carrier density $n=7 \times 10^{20}$ cm^{-3} prepared on a ZnO film (dashed curves). (c) Electron-density dependence of the Fermi-level shift, as obtained from the shift of the position of the main features identified in (a) and (b) with respect to these obtained in an nondegenerate film. Solid line is a $n^{2/3}$-linear fit of the experimental data.

converged with respect to the real space grid, the Brillouin zone sampling, and the range of the numerical atomic orbitals.

IV. RESULTS AND DISCUSSION

A. UPS results

Figures 1(a) and 1(b) show the UPS spectra measured in ZnO:Ga thin films deposited on sapphire with different electron concentration (n) by means of He I and He II radiation, respectively. The main features that can be identified correspond to the highest ZnO valence band, which is mainly derived from the O $2p$ orbitals, and the Zn $3d$ band.[34] These bands appear to be located at 4.41 and 10.76 eV from the E_F in a nondegenerate ZnO sample, respectively. As the ZnO conduction band populates, these features appear to progressively shift to higher binding energies. In order to follow the
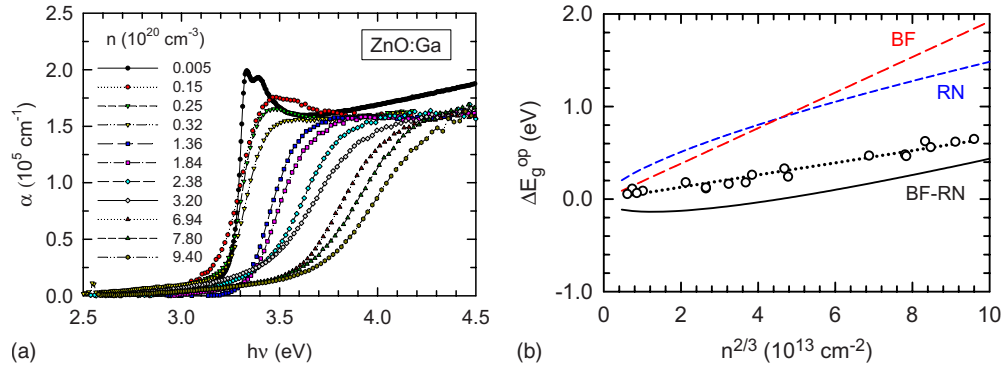
FIG. 2. (Color online) (a) Absorption edge measured at room temperature in ZnO:Ga films with different n up to 10^{21} cm^{-3}. (b) (circles) Optical band-gap shift observed in ZnO:Ga films as a function of n, as extracted from the absorption edge spectra showed in (a). The reference value of nondegenerate ZnO band gap is 3.34 eV. Dotted line is a fitting to the experimental data in the frame of the Burstein-Moss model. Solid curve (BF-RN curve) is the E_g^{op} shift with n expected in the frame of the standard filling model for n-doped ZnO. Dashed lines correspond to the band-filling (BF curve) and the band-gap-renormalization (RN curve) contributions to the E_g^{op} shift expected in the frame of this model.

evolution of the E_F with n, we have determined the energy position of the above-mentioned features by a Gaussian fitting procedure after background subtraction. Figure 1(c) shows the n dependence of the E_F shift with respect to the ZnO valence band and the Zn 3d band, as obtained from these fitting procedures. Both band shifts have been plotted together to stress that they exhibit similar carrier-concentration dependence. These results indicate that the E_F achieves an upshift of $\sim$0.4 eV at $n \approx 10^{21}$ cm^{-3}. It may be objected that the large dispersion of results of Fig. 1(c) may prevent an accurate determination of the E_F shift due to doping by UPS. This objection is based on the fact that UPS is a surface sensitive technique and the presence of surface defects may alter the E_F position at the surface with respect to that in the film. In our films, most of surface defects can be attributed to be originated by the sputtering process performed just before UPS measurements. Consequently, it would be desirable to use ZnO and ZnO:Ga films identically treated in order to determine the E_F shift caused by doping. This can be achieved by using ZnO:Ga/ZnO homojunctions in which a nondegenerate film is partially covered with a ZnO:Ga film deposited at the same conditions, being both films simultaneously sputtered. In Figs. 1(a) and 1(b), we have included the UPS spectra measured in the nondegenerate film and in the ZnO:Ga film with $n = 7 \times 10^{20}$ cm^{-3} of one of these homojunctions. Comparing these spectra, the E_F in this ZnO:Ga film appears to upshift by 0.4 eV with respect to that of the nondegenerate one, which agrees with the n dependence of the E_F measured in single ZnO:Ga thin films [Fig. 1(c)] and allows us to attribute the E_F observed by UPS to doping effects.

B. Ambient pressure optical results

Figure 2(a) shows the absorption edge of ZnO:Ga thin films with n up to 10^{21} cm^{-3}. The E_g^{op} was determined through the Elliott-Toyozawa theory,[35,36] as described in Ref. 16. This method leads to practically the same results as fitting a Gaussian to the first derivative of the absorption edge.[11] Figure 2(b) shows the E_g^{op}, as obtained through this

procedure, as a function of n. The E_g^{op} obtained for nondegenerate ZnO ($E_{go}^{\mathrm{op}} = 3.34$ eV) has been adopted as reference value. Consistently with other authors' results,[7,11] the E_g^{op} shifts to higher photon energies with increasing n, as the band filling effect (Burstein-Moss effect)[14,15] overcompensates the band-gap renormalization effect due to heavy doping.[6,13] In a pure band filling model, the E_g^{op} shift should be proportional to $n^{2/3}$. Results showed in Fig. 2(b) illustrate how the E_g^{op} seems to follow the Burstein-Moss theory, $\Delta E_g^{\mathrm{op}}(n) = E_g^{\mathrm{op}}(n) - E_{go}^{\mathrm{op}} = \hbar^2(3\pi^2 n)^{2/3}/2m_{eh}^*$, where $\hbar$ is the reduced Planck constant and m_{eh}^* is the electron-hole reduced mass ($1/m_{eh}^* = 1/m_e^* + 1/m_h^*$). A linear fit to the experimental results yields a value of $m_{eh}^* = 0.55m_o$, where m_o is the free electron mass, which is nearly three times higher than the actual value found in the literature.[6] This mass enhancement cannot be explained by nonparabolicity effects,[7] which suggests that the valence- and conduction-band contributions to the ΔE_g^{op} are lower than these expected from a band filling model. Both contributions can be estimated by combining UPS and optical results, since UPS results showed in Fig. 1(c) can provide direct information on the conduction-band contribution to the ΔE_g^{op}. At the highest n reached, the effective E_F shift observed is 0.4 eV [Fig. 1(c)] and the ΔE_g^{op} appears to be 0.60 eV [Fig. 2(b)]. Consequently, the corresponding conduction- and valence-band contributions to the ΔE_g^{op} result to be 0.37 and 0.23 eV at this doping stage, respectively, taking into account that the E_F is at some 30 meV below the conduction band in nondegenerate ZnO ($n \approx 10^{18}$ cm^{-3}). In a pure band filling model of ZnO, these contributions should be expected to be 1.25 and 0.59 eV, respectively, assuming $m_h^* = 0.59m_o$ and $m_e^* = 0.28m_o$.[6] These results evidence the inadequacy of the pure band filling model to explain the change of ΔE_g^{op} with n observed in ZnO, as has been already pointed out.[6,7]

The fact that the ΔE_g^{op} dependence on n observed in ZnO could not be explained by using a pure band filling model has been attributed to many-body effects including electron exchange interactions, minority-carrier correlations, and carrier-ion correlations.[6,13] These many-body effects enhance simultaneously with the band filling and tend to reduce the

magnitude of the ΔE_g^{op} caused by band filling. It has been proposed that these many-body interactions give rise to a band gap renormalization (ΔE_g^{RN}) which may be evaluated for *n*-ZnO as[13]

$$\Delta E_g^{\mathrm{RN}} = K_1 n^{1/3} + K_2 \left(\frac{m_e^*}{m_o}\right)^{1/4} n^{1/4} + K_3 \left(\frac{m_o}{m_e^*}\right)^{1/2} \left(1 + \frac{m_h^*}{m_e^*}\right) n^{1/2},$$

$$(1)$$

where each term accounts for electron exchange interactions, minority-carrier correlations, and carrier-ion correlations, respectively. The corresponding K_i coefficients depend on physical constants of the semiconductor, which can be obtained to be $K_1 = 2.66 \times 10^{-8}$ eV cm, $K_2 = 8.53 \times 10^{-7}$ eV cm$^{3/4}$, and $K_3 = 5.96 \times 10^{-12}$ eV cm$^{3/2}$ for ZnO.[13] In this way, we have calculated the ΔE_g^{RN} as a function of *n* expected in the frame of this model, as well as the contribution to the ΔE_g^{op} corresponding to the band filling. The results of these calculations are shown in Fig. 2(b) (dashed lines) which give rise to effective ΔE_g^{op} values [solid line in Fig. 2(b)] whose variation with *n* resembles to that obtained experimentally. However, they appear to underestimate the current optical gap values measured and even to give negative ΔE_g^{op} values at low *n*. This fact is a consequence of the surprisingly high value of $\Delta E_g^{\mathrm{RN}} = 0.2$ eV calculated for the lowest *n* reached, which seems to be related to the inadequacy of these models for a weakly degenerate electron gas.[37] Besides these facts, the calculated ΔE_g^{op} values fail also to describe the experimental ones obtained in heavily doped films, for whose *n* these models were proposed.

C. Optical measurements under high pressure

The facts evidenced in the previous subsection indicate that the relative contribution of the band-filling and band-gap-renormalization mechanisms to ΔE_g^{op} should be revised even at high *n*. In order to approach this task, an experimental determination of each one of these contributions would be required. Band-filling and band-gap-renormalization contributions are difficult to be separated by means of current experiments in which temperature or doping is varied. However, this can be achieved by considering the pressure as a new variable to be exploited. With this aim, optical measurements of the absorption edge have been performed in free-standing ZnO:Ga films with different *n* under pressure. Proceeding as before, we have determined the E_g^{op} of these films, which are shown in Fig. 3 as a function of pressure. These results reflect a linear variation of the E_g^{op} with pressure for all films studied, whose pressure coefficients are summarized in Table I. These results indicate that the pressure coefficient of the E_g^{op} decreases as *n* increases. This fact may be tentatively attributed to effects of pressure on *n*. However, transport measurements under pressure showed that *n* is constant while samples remain in the wurtzite phase (below 9.5 GPa).[38] Therefore, the fact that the *n* dependence of the E_g^{op} is sensitive to pressure (Fig. 3) suggests that the two competing effects (band filling and band-gap renormalization) change their relative weight under pressure. This fact would allow us to estimate their absolute values at ambient pres-
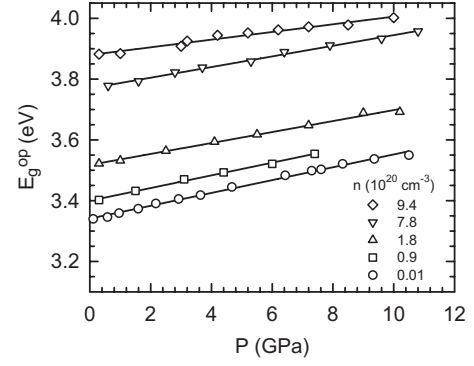
FIG. 3. Pressure dependence of the optical band gap, as extracted from optical measurements carried out in free-standing ZnO:Ga films with different *n*. Solid lines are linear fit to the experimental data.

sure. Let us call $\Delta E_g^{\mathrm{op}}(0)$ and $\Delta E_g^{\mathrm{op}}(P)$ to the optical gap shifts at ambient pressure and at a given pressure *P*, respectively. The ratio between them can be written as

$$\frac{\Delta E_g^{\mathrm{op}}(P)}{\Delta E_g^{\mathrm{op}}(0)} = \frac{\Delta E_g^{\mathrm{BF}}(P) - \Delta E_g^{\mathrm{RN}}(P)}{\Delta E_g^{\mathrm{BF}}(0) - \Delta E_g^{\mathrm{RN}}(0)} = \frac{\alpha - \beta y}{1 - y},$$

$$(2)$$

where $\Delta E_g^{\mathrm{BF}}(P)$ and $\Delta E_g^{\mathrm{RN}}(P)$ stand for the band filling and band gap renormalization contributions at *P*, $\alpha = \Delta E_g^{\mathrm{BF}}(P) / \Delta E_g^{\mathrm{BF}}(0)$, $\beta = \Delta E_g^{\mathrm{RN}}(P) / \Delta E_g^{\mathrm{RN}}(0)$, and $y = \Delta E_g^{\mathrm{RN}}(0) / \Delta E_g^{\mathrm{BF}}(0)$. The pressure dependence of the physical quantities involved in $\Delta E_g^{\mathrm{BF}}(P)$ and $\Delta E_g^{\mathrm{RN}}(P)$ can be found in the literature.[39,40] $\Delta E_g^{\mathrm{BF}}(P)$ is determined by the effective mass, whereas $\Delta E_g^{\mathrm{RN}}(P)$ depends on the effective mass, dielectric constant, and compressibility.[13] As an example, let us calculate the contribution of each effect for a ZnO:Ga 5% film with *n* $= 9.4 \times 10^{20}$ cm^{-3} (top curve in Fig. 3). For $P = 10$ GPa, the $\Delta E_g^{\mathrm{op}}(P) / \Delta E_g^{\mathrm{op}}(0)$ ratio is 0.838 and the other parameters in Eq. (2) can be calculated from data in the literature ($\alpha = 0.939$ and $\beta = 0.996$).[39,40] With these values of α and β, Eq. (2) yields $y = 0.639$. Since the ΔE_g^{op} obtained at ambient pressure is 0.60 eV [Fig. 2(b)] the band filling and band-gap-renormalization contributions turn out to be 1.66 eV and 1.06 eV, respectively. This band filling contribution could be separated into these corresponding to the conduction and valence bands, which would be 1.12 eV and 0.54 eV, respectively, attending to their respective effective-mass weight. By

TABLE I. Pressure coefficient of the optical gap obtained for ZnO:Ga films. The nominal Ga content as well as the carrier density of each film are indicated.

Ga content (%)	n (10^{20} cm^{-3})	Pressure coefficient (meV/GPa)
Nondegenerate	~ 0.01	21.1 ± 0.4
0.25	0.9	20.9 ± 0.7
0.5	1.8	18.1 ± 0.6
2.5	7.8	17.5 ± 0.5
5.0	9.4	12.6 ± 0.8
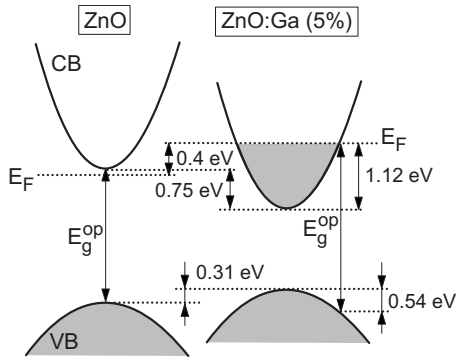
FIG. 4. Summary of the band-filling and band gap renormalization contributions to the ΔE_g^{op} obtained experimentally for a ZnO:Ga 5% film with $n = 9.4 \times 10^{20}$ cm^{-3}.

combining these results with those reported above (Figs. 1 and 2) a detailed quantification of the contribution of each mechanism to the ΔE_g^{op} produced by doping can be obtained, which has been summarized in Fig. 4 for the highest doping reached. This scheme would allow us to identify the reasons why standard models of ΔE_g^{op} fail when applied to ZnO. At the highest n reached, the band-gap renormalization contribution from the conduction and valence bands appears to be 0.75 eV and 0.31 eV, respectively (Fig. 4). These two band-gap renormalization contributions should be expected to be 0.61 eV and 0.84 eV by using Eq. (1), respectively. Then, it appears that the band-gap renormalization contribution coming from holes is largely overestimated by using standard models. This term is mainly determined by hole-ion correlations, which suggests that the interaction of holes with donors may be screened in a larger degree than that predicted by standard models. With regard to the band-filling contribution, that attributed to the valence band (Fig. 4) seems to be quite well reproduced by that expected from the Burstein-Moss model (0.59 eV). However, it can be seen that the conduction-band term is smaller than that predicted (1.25 eV), which can be attributed to nonparabolicity effects in the conduction band.

Nonparabolicity effects have been invoked in order to explain the n dependence of the ΔE_g^{op}.[7,41] Obviously, the nonparabolicity parameters used in these estimations are those of pure ZnO.[7] In this context, it will be expected that nonparabolicity effects become important at high n, but irrespective to the cation selected to dope ZnO. Consequently, ZnO:M films prepared with any M element from the group III should exhibit the same evolution of the ΔE_g^{op} with n. ZnO:Al films appear to exhibit an evolution of the ΔE_g^{op} with doping that resembles to that obtained here for ZnO:Ga films.[6] However, a detailed inspection of these two ΔE_g^{op} evolutions [see also Fig. 5(b)] reveals that the n required to obtain a ΔE_g^{op} of ~0.5 eV in ZnO:Ga is twice that needed for ZnO:Al. In spite of this observation, experimental uncertainties are still quite large to reach a definitive conclusion.[6] In order to contribute to the understanding of the chemical role of group-III elements, we have measured the absorption edge of ZnO:In films with different n, which are shown in Fig. 5(a). Proceeding as before, the E_g^{op} of these films has been determined through the Elliott-Toyozawa model of the absorption
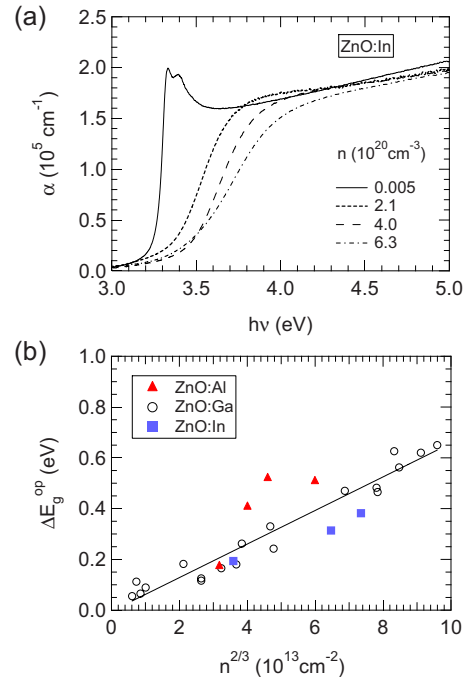
FIG. 5. (Color online) (a) Absorption edge measured at room temperature in ZnO:In films with different n up to 7×10^{20} cm^{-3}. (b) Optical band gap shift of ZnO:In films as a function of n, as extracted from the absorption edge spectra showed in (a). The reference value of nondegenerate ZnO band gap is of 3.34 eV. Data from Fig. 2(b) (open circles) as well as from Ref. 6 (triangles) have been reproduced here for comparison. Solid line is a $n^{2/3}$-linear fit of the experimental data obtained for ZnO:Ga, to guide the eye.

edge.[35,36] The E_g^{op} obtained for these ZnO:In films is shown in Fig. 5(b) as a function of n. In this figure, we have included, for comparison, the results obtained here for ZnO:Ga [Fig. 2(b)] as well as those already reported for ZnO:Al films.[6] From these results, it can be seen that, beyond a certain n, the E_g^{op} obtained for ZnO:In films are clearly ~0.1 eV below those of ZnO:Ga, at the same n. These results are indicative that these cations tend to perturb the ZnO conduction band, with the interaction strength increasing in going from Al to Ga to In. As a consequence of this interaction, it appears that the nonparabolicity of the conduction band is enhanced in these films.

D. Density-functional calculations

Some close examples of how heavy doping strongly perturbs the band structure of the host semiconductor can be found in literature. Mryasov et al.[42] carried out a full-potential linear muffin-tin orbital calculation of the band structure of indium-tin oxide. By replacing one of the 16 In atoms of the In_2O_3 unit cell by a tin atom, a gap appeared to open in the conduction band immediately above the E_F. This gap was found to originate from the interaction between In_2O_3 conduction-band states and the antibonding state of the Sn-O bond, a localized state related to Sn. Motivated by these results, we have performed DFT calculations of the band structure of ZnO:M for a dopant content of 3% (see Sec. III for details). The band structure calculated for
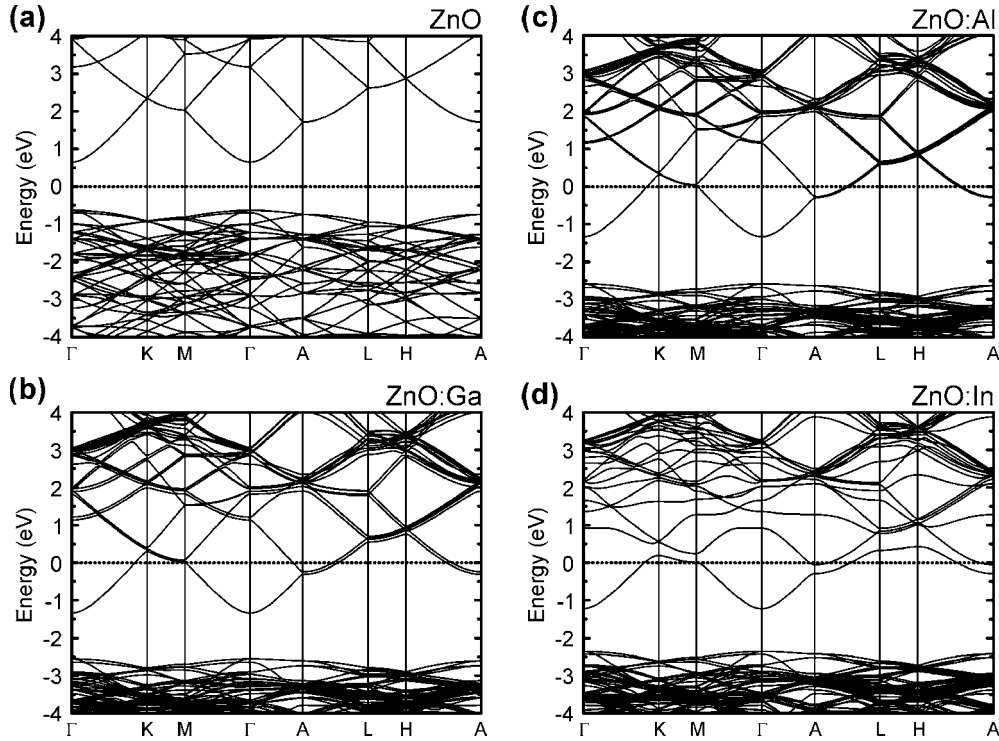
FIG. 6. Band structure of (a) pure ZnO, (b) ZnO:Ga, (c) ZnO:Al, and (d) ZnO:In calculated by the DFT method along various directions of the ZnO Brillouin zone by using a $3 \times 3 \times 2$ supercell. In order to simulate heavy doping, a dopant content of 3% has been selected in these calculations. In all plots, the dotted line at 0 eV indicates the Fermi-level position.

ZnO:M 3% are showed in Fig. 6, in which that calculated for pure ZnO has been also included for comparison. These results clearly reflect features expected for heavily doped ZnO. On one side, the E_F is located well inside the ZnO conduction band, at some 1.3 eV above its minimum, as would be expected for a degenerate semiconductor. On the other side, the energy gap existing between the valence and conduction bands in ZnO is kept in heavily doped ZnO (with the usual DFT underestimation). This accounts for semiconducting features remaining in heavily doped ZnO as the fact that the optical gap occurs at photon energies corresponding to the optical transition between states whose wave vector **k** is the Fermi wave vector. Even if these effects can be readily explained within a simple doping scheme, the fact that small gaps appear in the electronic structure of ZnO:M at specific points of the Brillouin-zone border (at the K, M, A, L, and H points) makes this doping model no longer valid. Similarly to that found for In$_2$O$_3$:Sn,[42] these gaps appear as a consequence of the fact that dopants introduce localized antibonding states (thus modifying the symmetry properties of the system) that perturb the ZnO conduction band. However, these gaps do not cover the whole Brillouin zone as it was found for In$_2$O$_3$:Sn.[42] It should be stressed that in the calculations performed in Ref. 42 the Sn concentration was twice that used here and that our results clearly show the trend of the gaps to grow as the dopant content is increased.

Although this interaction does not open a gap that covers the whole Brillouin zone, it is enough to modify the conduction-band dispersion and the magnitude of the ΔE_g^{op} that would be expected by the standard models for ZnO:$\tilde{M}$. This effect of the interaction is illustrated in Fig. 7. Metal

atoms lead to the introduction of localized states of energy E_s into the ZnO band structure that interact with the ZnO conduction band $E_c(\mathbf{k})$. The interaction leads to a mixing and anticrossing of these two bands, which opens a gap in the ZnO conduction band and gives rise to perturbed bands of energy $E_\pm(\mathbf{k})$. After inclusion of the interaction, the n remains unaltered (Luttinger theorem).[43] Therefore, the magnitude of the ΔE_g^{op} is reduced when the optical transition promotes electrons from the valence band to states in the conduction band close to the new gap, i.e., at sufficiently high doping. This scheme establishes a direct connection between the magnitude of the new gap and its consequent re-
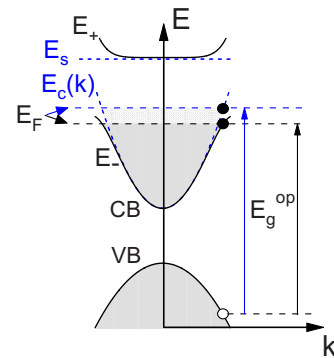
FIG. 7. (Color online) Illustration of the interaction occurring between a localized state of energy E_s and the conduction band with band dispersion $E_c(\mathbf{k})$, which are plotted in dashed blue lines. The mixed bands [$E_\pm(\mathbf{k})$], resulting for the interaction, are indicated in solid lines. As a consequence of the interaction, the magnitude of the ΔE_g^{op} is reduced.

duction of the ΔE_g^{op}. From our band structure calculations (Fig. 6), it can be seen that the interaction degree depends on the metal choice. In fact, the gap is almost negligible for ZnO:Al 3% whereas, for ZnO:In 3%, it is three times larger than that found for ZnO:Ga 3%. Therefore, these results would qualitatively explain experimental results obtained here for ZnO:Ga and ZnO:In as well as why standard models appear still to be a quite valid framework to understand the E_g^{op} evolution with n in ZnO:Al,[6,7] at least in the n range reported.

E. Band-anticrossing model approach

In order to test whether the above described interaction can quantitatively account by itself for the differences in the ΔE_g^{op} values obtained for each ZnO:M film at high doping, we will use the above described standard model. As it has been already mentioned, this model underestimates the absolute value of the E_g^{op} in ZnO:M, but it may provide for a reasonable estimate of relative variations in the ΔE_g^{op} when the interaction is considered. In order to face this task, the enhancement of the m_e^* owed to the interaction must be evaluated. For this purpose, we have simulated conduction-band changes through a perturbation theory model as that adopted in the band-anticrossing interaction,[44] schematized in Fig. 7. In this framework, the Hamiltonian of the interacting system would be

$$H = \sum_{\mathbf{k}\sigma} E_c(\mathbf{k})c_{\mathbf{k}\sigma}^{\dagger}c_{\mathbf{k}\sigma} + E_s a_{\mathbf{k}\sigma}^{\dagger}a_{\mathbf{k}\sigma} + V(c_{\mathbf{k}\sigma}^{\dagger}a_{\mathbf{k}\sigma} + a_{\mathbf{k}\sigma}^{\dagger}c_{\mathbf{k}\sigma}),$$

(3)

where σ is the spin quantum number. The first term describes the unperturbed conduction band, the second one represents electrons in the localized metal-O related state, and the last accounts for the interaction between these two bands, with energy V. As it has been suggested,[45] the interaction energy V may depend on n. We have adopted $V = V_o n(\mathrm{cm}^{-3})/10^{21}$, where V_o is an energy, independent of $\mathbf{k}$ for simplicity. In this way, the band dispersion of the interacting bands ($E_\pm$) can be obtained by diagonalizing the Hamiltonian of Eq. (3) as

$$E_\pm(\mathbf{k}) = \frac{E_c(\mathbf{k}) + E_s}{2} \pm \frac{1}{2}\sqrt{(E_c(\mathbf{k}) - E_s)^2 + 4V^2}. \quad (4)$$

The effective mass of the perturbed conduction band (m_e^{**}) would be $\mathbf{k}$ dependent, which may be calculated to be

$$\frac{1}{m_e^{**}(\mathbf{k})} = \frac{1}{2m_e^*}\left[1 + \frac{|E_s - E_c(\mathbf{k})|}{\sqrt{(E_c(\mathbf{k}) - E_s)^2 + 4V^2}}\right]. \quad (5)$$

In the framework of this interaction model, $E_s - E_c(\mathbf{k}=0)$ and V_o must be evaluated. In the case of ZnO:In [Fig. 6(d)] the gap clearly opens at ~ 1.5 eV from the bottom of the conduction band, then, it seems reasonable to assume that $E_s - E_c(\mathbf{k}=0) \approx 1.5$ eV. With this $E_s - E_c(\mathbf{k}=0)$ value, V_o would determine the size of the gap opening at the conduction band. In ZnO:In 3%, the conduction band seems to downshift by 0.3 eV at the zone border with respect to that of pure ZnO [Fig. 6(a)] which appears to be reproduced by
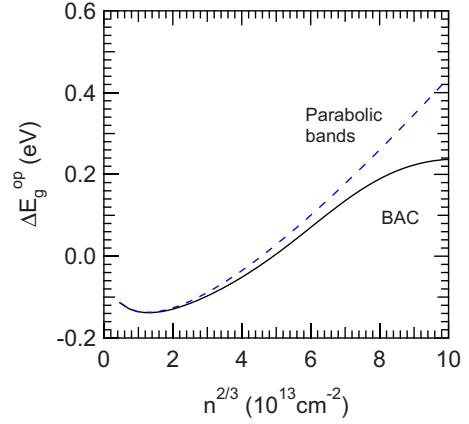
FIG. 8. (Color online) Optical band gap shift calculated as a function of n by considering parabolic bands (dashed blue line) and a band-anticrossing model (BAC curve).

taking $V_o = 0.8$ eV. In this way, we have calculated the ΔE_g^{op} as a function of n by considering the enhancement of the m_e^* expected by using Eq. (5) for ZnO:In. The results of these calculations are showed in Fig. 8, where the ΔE_g^{op} expected in the case of unperturbed bands has been included, for comparison. These results reflect that, when the interaction is considered, the magnitude of the ΔE_g^{op} can be reduced even by ~ 0.2 eV at the highest doping reached. This reduction in the ΔE_g^{op} is mainly originated by the lesser band-filling contribution to the ΔE_g^{op} when nonparabolic bands are considered. These results are consistent with the behavior observed for ZnO:In films [Fig. 5(b)] and indicate that chemical effects must be taken into account to quantitatively explain the ΔE_g^{op} produced in heavily doped ZnO films prepared by using elements from the group III.

Finally, a word should be said about the fact that elements from the group III introduce localized levels that interact with the ZnO conduction band in a different degree. This fact can be readily understood in the frame of the band-anticrossing model [Eq. (4)]. It would be expected that the energetic position of the localized M-O antibonding states into the ZnO band structure were correlated with the band-gap value of the M_2O_3 oxides, since the valence band of both these oxides and ZnO mainly derives from O $2p$ orbitals and the conduction band in the oxides stems from metal s orbitals. In these oxides, the band gap decreases in going from Al_2O_3 to Ga_2O_3 to In_2O_3.[46–48] Following this sequence, the localized states introduced in ZnO:In would be closer to the ZnO conduction-band minimum than these introduced in ZnO:Al. Therefore, Al would be expected to perturb the ZnO conduction band only at very high doping, probably beyond the n range approached in early studies,[6] whereas the interaction effects in ZnO:In films become appreciable at the doping degree reached in this work.

V. SUMMARY

In this work we have analyzed chemical effects on the optical-band-gap evolution with doping in heavily n-doped ZnO:M films (M=Al, Ga, and In). By combining valence-

band photoemission measurements as well as optical measurements of the absorption edge performed as a function of doping and pressure, the different contributions to the optical-band-gap shift observed with doping have been quantitatively determined, in particular, for ZnO:Ga thin films. These results appear to give experimental evidence that standard models usually evoked to explain optical band-gap shifts with doping seem to fail when applied to these films. These models are based on the Burstein-Moss theory partially compensated by band-gap renormalization effects, in which it has been assumed that the electronic structure of the host semiconductor remains unaltered in the doped material. In order to test the validity of this assumption, we have extended this study to ZnO films heavily doped with other group-III elements. The absorption edge measured in ZnO:In films as a function of doping reflected a lower increase of the optical-band-gap shift with doping than that observed in ZnO:Ga. The behavior observed for these two kinds of films contrasts with that already reported for ZnO:Al. These results evidenced that chemical effects cannot be neglected and that depend on the cation choice.

In order to identify the origin of the different behavior of the band-gap-evolution observed with doping in these different films, their band structures have been calculated by using a numerical atomic orbitals density-functional theory approach. These calculations showed that metals introduce quite-localized antibonding metal-O states. These states appear to hybridize with the ZnO conduction band, opening a gap in the conduction band. However, the strength of the interaction depends on the element used to dope ZnO, which increases in going from Al to Ga to In. These results have been explained in the frame of a band-anticrossing model of the interaction. This band-anticrossing scheme agrees with experimental results reported here and with previous studies performed in heavily doped ZnO.

ACKNOWLEDGMENTS

*juan.f.sanchez@uv.es

[1] H. Ohta, K. Kawamura, M. Orita, N. Sarukura, M. Hirano, and H. Hosono, Electron. Lett. **36**, 984 (2000).

[2] X.-L. Guo, J.-H. Choi, H. Tabata, and T. Kawai, Jpn. J. Appl. Phys., Part 2 **40**, L177 (2001).

[3] V. Assunção, E. Fortunato, A. Marques, A. Gonçalves, I. Ferreira, I. Águas, and R. Martins, Thin Solid Films **442**, 102 (2003).

[4] S. J. Henley, M. N. R. Ashfold, and D. Cherns, Surf. Coat. Technol. **177-178**, 271 (2004).

[5] F. Pan, C. Song, X. J. Liu, Y. C. Yang, and F. Zeng, Mater. Sci. Eng. R. **62**, 1 (2008).

[6] B. E. Sernelius, K. F. Berggren, Z. C. Jin, I. Hamberg, and C. G. Granqvist, Phys. Rev. B **37**, 10244 (1988).

[7] H. Fujiwara and M. Kondo, Phys. Rev. B **71**, 075109 (2005).

[8] A. P. Roth, J. B. Webb, and D. F. Williams, Phys. Rev. B **25**, 7836 (1982).

[9] D. C. Reynolds, D. C. Look, and B. Jogai, J. Appl. Phys. **88**, 5760 (2000).

[10] A. Yamamoto, T. Kido, T. Goto, Y. Chen, and T. Yao, Solid State Commun. **122**, 29 (2002).

[11] T. Makino, Y. Segawa, S. Yoshida, T. Tsukazaki, A. Ohtomo, and M. Kawasaki, Appl. Phys. Lett. **85**, 759 (2004).

[12] J. D. Ye, S. L. Gu, S. M. Zhu, S. M. Liu, Y. D. Zheng, R. Zhang, and Y. Shi, Appl. Phys. Lett. **86**, 192111 (2005).

[13] S. C. Jain, J. M. McGregor, and D. J. Roulston, J. Appl. Phys. **68**, 3747 (1990).

[14] E. Burstein, Phys. Rev. **93**, 632 (1954).

[15] T. S. Moss, *Optical Properties of Semiconductors* (Butterworths, London, 1961).

[16] J. A. Sans, A. Segura, J. F. Sánchez-Royo, V. Barber, M. A. Hernández-Fenollosa, and B. Marí, Superlattices Microstruct. **39**, 282 (2006).

[17] J. A. Sans, A. Segura, M. Mollar, and B. Marí, Thin Solid Films **453-454**, 251 (2004).

[18] R. Letoullec, J. P. Pinceaux, and P. Loubeyre, High Press. Res. **1**, 77 (1988).

[19] G. J. Piermarini, S. Block, J. D. Barnett, and R. A. Forman, J. Appl. Phys. **46**, 2774 (1975).

[20] P. Hohenberg and W. Kohn, Phys. Rev. **136**, B864 (1964); W. Kohn and L. J. Sham, *ibid.* **140**, A1133 (1965).

[21] J. M. Soler, E. Artacho, J. D. Gale, A. García, J. Junquera, P. Ordejón, and D. Sánchez-Portal, J. Phys.: Condens. Matter **14**, 2745 (2002).

[22] For more information on the SIESTA code visit http://www.uam.es/siesta/

[23] For a review on applications of the SIESTA approach to materials science see D. Sánchez-Portal, P. Ordejón, and E. Canadell, Struct. Bonding (Berlin) **113**, 103 (2004).

[24] J. P. Perdew, K. Burke, and M. Ernzerhof, Phys. Rev. Lett. **77**, 3865 (1996).

[25] N. Troullier and J. L. Martins, Phys. Rev. B **43**, 1993 (1991).

[26] L. Kleinman and D. M. Bylander, Phys. Rev. Lett. **48**, 1425 (1982).

[27] S. G. Louie, S. Froyen, and M. L. Cohen, Phys. Rev. B **26**, 1738 (1982).

[28] E. Artacho, D. Sánchez-Portal, P. Ordejón, A. García, and J. M. Soler, Phys. Status Solidi B **215**, 809 (1999).

[29] N. A. Spaldin, Phys. Rev. B **69**, 125201 (2004).

[30] E. Anglada, J. M. Soler, J. Junquera, and E. Artacho, Phys. Rev. B **66**, 205101 (2002).

[31] B. Meyer, H. Rabaa, and D. Marx, Phys. Chem. Chem. Phys. **8**, 1513 (2006).

[32] E. H. Kisi and M. M. Elcombe, Acta Crystallogr. C **45**, 1867 (1989).

[33] H. J. Monkhorst and J. D. Pack, Phys. Rev. B **13**, 5188 (1976).

[34] L. Ley, R. A. Pollak, F. R. McFeely, S. P. Kowalczyk, and D. A. Shirley, Phys. Rev. B **9**, 600 (1974).

[35] R. J. Elliott, Phys. Rev. **108**, 1384 (1957).

[36] Y. Toyozawa, Prog. Theor. Phys. **20**, 53 (1958).

[37] S. C. Jain and D. J. Roulston, Solid-State Electron. **34**, 453 (1991).

[38] A. Segura, J. A. Sans, D. Errandonea, D. Martinez-García, and V. Fages, Appl. Phys. Lett. **88**, 011910 (2006).

[39] A. Mang, K. Reimann, and St. Rübenache, Solid State Commun. **94**, 251 (1995).

[40] F. Decremps, J. Pellicer-Porres, A. M. Saitta, J. C. Chervin, and A. Polian, Phys. Rev. B **65**, 092101 (2002).

[41] A. V. Singh, R. M. Mehra, A. Yoshida, and A. Wakahara, J. Appl. Phys. **95**, 3640 (2004).

[42] O. N. Mryasov and A. J. Freeman, Phys. Rev. B **64**, 233111 (2001).

[43] J. M. Luttinger, Phys. Rev. **119**, 1153 (1960).

[44] W. Shan, W. Walukiewicz, J. W. Ager, E. E. Haller, J. F. Geisz, D. J. Friedman, J. M. Olson, and S. R. Kurtz, Phys. Rev. Lett. **82**, 1221 (1999).

[45] J. Wu, W. Shan, and W. Walukiewicz, Semicond. Sci. Technol. **17**, 860 (2002).

[46] J. Guo, D. E. Ellis, and D. J. Lam, Phys. Rev. B **45**, 13647 (1992).

[47] M. Passlack, E. F. Schubert, W. S. Hobson, M. Hong, N. Moriya, S. N. G. Chu, K. Konstadinidis, J. P. Mannaerts, M. L. Schnoes, and G. J. Zydzik, J. Appl. Phys. **77**, 686 (1995).

[48] R. L. Weiher and R. P. Ley, J. Appl. Phys. **37**, 299 (1966).